

Fracture Physics in Comminution

Hans Rumpf, Karlsruhe

In connection with structural design and in the study of material behaviour the discipline of fracture mechanics usually has two aims: On the one hand one is interested in avoiding failures through fractures and on the other hand in better understanding the ways by which cracks can develop in construction materials under different loading conditions. The basic question to be answered is usually whether fracture propagation is possible, and if it is possible, whether a definite time lapse is associated with the onset of rapid fracture; for it is of greater engineering interest in most designs to determine when fracture propagation begins, rather than investigate the relatively short time span during which the final failure occurs due to rapid crack extension. One distinguishes two primary uses of fracture mechanics:

- 1.) To obtain in better understanding of the physics of fracture, and
- 2.) to develop tests which promote a deeper and more comprehensive knowledge of the behaviour of the engineering materials.

As a consequence of these uses one chooses test conditions and materials which permit a relatively precise determination of the deformation and stress fields during the fracture process, or at least a reasonably good estimate.

In connection with comminution the discipline of fracture mechanics should have an equal or even greater importance since comminution uses the fracture process to make small particles from larger ones.

But the situation of fracture mechanics to be used for better engineering in comminution is much more difficult

and complicated than with construction materials. The reasons are the following:

- 1.) Particles to be comminuted, normally are of irregular shape. They are often produced by a preceding comminution process or by crystallization, condensation, drying or sintering.
- 2.) Most materials to be comminuted are not isotropic, but polycrystalline and inhomogeneous, and possess initial flaws of unknown distribution in size and orientation.
- 3.) In a grinding machine the particles are collectively handled: There is a broad spectrum of loading conditions and intensities which can act on individual particles. Many particles may not be loaded at all and others again experience an excess of energy of deformation. It is one of the engineering problems to determine the optimum loading conditions and then to realize them most uniformly for all particles.
- 4.) The criteria by which optimal loading is achieved are not governed only by efficient fracturing but also by the requirement to produce fragments with special properties at a minimum of cost. Such properties are for instance: the chemical reactivity, the liberation of ores, the optical qualities of pigments, taste and colour of foodstuff, the effectiveness of drugs, the rheological and other handling properties. All of these depend on the particle size distribution and the shape of the fragments, as well as on their specific surface properties and the surface state. Thus it is not only the initial phase of the fracture process but its complete execution which produces the fracture pattern and the surface state which determines the result of comminution.

What can we do with fracture mechanics under these circumstances? The comminution techniques have been developed empirically. Machinery exploiting these techniques already exist and we cannot expect to upstage these empirical and working methods of a long lasting development. But we can expect to improve these methods by applying developments which are more efficient than empiricism. In order to improve them it is useful to understand the physical mechanism and fracture mechanics and fracture physics are necessary for that purpose. But there is a great gap in knowledge between the understanding of fracture physics in a tensile test and the quantitative prediction of fracture phenomena in collective grinding of irregularly shaped particles. We try to fill up this gap by the following steps [1,2]:

- 1.) Examination of fracture phenomena in regularly shaped particles, mainly spheres, under definite loading conditions which are similar to those in practical comminution. These are
 - a) Compression of single particles and a bed of particles, respectively, between plane or spherical surfaces
 - b) impacting of particles against surfaces large compared to the particle size or against other particles, and
 - c) stressing of particles in a fluid as, for example, in a shear flow.
- 2.) Studying the fracture phenomena in irregularly shaped particles under the same definite loading conditions as in 1).

These investigations should be analytical as far as possible, but the main effort tends to be experimental. In our own experience we found it absolutely necessary to develop

instrumentation which accomodates the wide particle size spectrum from 1 μm to 10 cm^*). In addition one must be able to work with a large range of rheological behaviours to encompass such diverse materials as diamond and wax, soft rubber, including temperature sensitive materials, fibrous materials, agglomerates and inhomogeneous particles.

B. Fracture phenomena in spheres by compression and impact loading

B.1 Compression loading

Here we may distinguish three cases.

Purely elastic deformation before fracturing.

One observes experimentally that ring-cracks develop in the zone of maximum tensile stresses at the periphery of the contact circle and propagate along the σ_1 -trajectory of the Hertz-Huber stress field (Fig. 1) [3], perpendicular to the maximum tensile stresses σ_2 . The σ_2 -stresses decrease very much along the σ_1 -trajectory, as shown in Fig. 2 [3]. An equilibrium results between crack extension force and fracture surface energy at a certain crack length, if the load remains constant. Wilshaw and Hartley [4] have developed a relationship for this situation.

With rising load, the contact circle increases and the σ_1 -trajectory, which previously startet in the tensile stress region now moves into the growing compression stress region associated with the contact zone. The ring crack may stop before having reached the stable length. A new ring crack can be caused outside the contact circle and in this way a series of small ring cracks is developed. But at a certain load the last crack can propagate fast up to the stable

*) This work is going on in Dr. Schönerts group on our Laboratory with the help of the "Stiftung Volkswagenwerk".

crack length. We have observed to different types of stable cone cracks: a centre-near and a surface-near form (Fig. 3) [3]. The centre-near cone crack occurs more often in connection with higher loading velocities. These cone cracks do not destroy the sphere, they merely grow toward to the surface and split off small fragments.

A further increase of the force causes the rapid destruction of the sphere as shown in the sequence of high speed photographs in Fig. 4 [3]. These cracks start on the divergent surface formed by the cone crack, with the ring cracks probably serving as initial flaws. With increasing elastic energy stored before total destruction more cracks are developed. Away from the initial fracture zone the cracks follow approximately the stress trajectories of the undistorted sphere, forming thin fragments like layers of an onion. Crack velocities up to 2300 m/s, were measured which is much higher than the maximum crack velocity in glass observed to date in tensile tests. The conclusions is, that the maximum crack velocity depends on the stress state. In a sphere the cracks are propagated into a converging stress field.

Cracks generated in an elastic stress field induced by plastic deformation.

Fig. 5 [3] shows a half sphere which was split as the result of a compression test. Beneath the contact area a cone has been sheared into the material and caused peripheral tensile stresses in agreement with plasticity theory. These stresses cause cracks in meridian planes and the wax half sphere has been split by this type of crack. Fig. 6 [3] shows the contact circle and the surrounding area of a polystyrene sphere, which has been compressed. Both crack phenomena discussed so far can be observed: ring cracks caused by the σ_2 -tensile stresses of the Hertz-Huber stress field and radial-meridial fractures, caused by perpherical σ_3 -tensile stresses associated with

plastic deformation. In the pure Hertz-Huber stress state, the σ_3 -stresses in region III (Fig. 1) are tensile stresses, but of small amplitude; they can be amplified through plastic deformation and cracks may then start at flaws within a sphere (Fig. 7) [3] .

Cracks generated during or after unloading.

When the deformations are purely elastic the σ_3 -stresses in region I and II (Fig. 1) are compressive. The plastic deformation causes the σ_3 -stresses to become increasingly tensile. Both are superimposed and the resulting σ_3 -stress may be smaller than the maximal σ_2 -tensile stress. If the load is then removed, the residual σ_3 -stresses, caused by the irreversible deformation, may be tensile stresses and high enough to cause cracks in materials with high strength. This is typical for small glass spheres, which have a very high fracture strength and, as a consequence are prone to deform plastically. It may thus be argued, that unloading fracturing plays a rather important role in comminution especially of fine particles with high strength.

B.2 Impact loading of spheres

In an impacted sphere different kinds of stress waves are generated at the impact center and sweep through the body: one observes compression and tensile waves, as well as surface waves. The primary compression wave moves the material points to larger radii thereby inducing these tensile stresses perpendicular to the wave front, which are called the dynamic hoop-stresses. These hoop-stresses produce cracks diverging from the impact center into the sphere following the elastic wave front. It is also possible that there exist some cracks initiated at special interior points, where the interfering reflected waves produce large tensile stresses. Such a tensile stress maximum is found on the impact axis, three quarters of the diameter away from the impact point. These possibilities

have been studied theoretically and experimentally by Gildemeister and Schönert [5] . Fig. 8 shows several high speed photographs of an impacted plexiglass disk which serves as a two-dimensional analog for the sphere. The main fracture field near the impact point is created by the "hoop-stresses" spreading out from the contact zone. The dark spot at the place of the maximum of the reflected tensile stresses indicates a local fracture.

C. Fracture phenomena in irregularly shaped particles

Only a few typical phenomena are described below which are important for the understanding of the following chapter.

C.1 Particles deform mainly elastically

Fig. 9 shows load-displacement curves of a 38 μm glass sphere and of an about 130 μm irregularly shaped quartz particle measured in our micro compression testing equipment [6] . The glass sphere is stressed elastically and shatters at a certain load. The quartz particle experiences many brittle fractures, which cause small fragments to fly off or cracks to run into the material. The final result is a very large number of fragments of different sizes down to less than one micron. The smallest fragments which could be detected were of 0.02 μm in size.

C.2 Particles deform elastically and plastically

One finds that particles of "brittle" material deform not only elastically but also plastically if they are small enough. For example Fig. 10 [7] shows a scanning electron micrograph of a 9 μm limestone particle after compression loading. The contact face is flattened, strong plastic deformation having occurred. The tendency of small particles to deform plastically can be understood from fracture mechanics. The probability of existing initial flaws in the region of maximum tensile stresses which are large enough for crack initiating, decreases with decreasing stressed volume; therefore the chance increases, that the shear

stresses can cause plastic deformations before fracturing. But brittle fracturing still occurs as can be seen in Fig. 10.

C.3 Particles deform mainly plastically

Fig. 11 shows the load-displacement-curve of a 1.7 μm quartz particle. The curve is smooth and sudden load drops which normally indicate fracturing are absent. The unloading curve is much steeper, and irreversible deformation of about 0.5 μm, i.e. a third of the particle size, has taken place: the particle was plastically flattened in compression. Superficially it seems that no fracturing has occurred but the two scanning electron micrographs show cracks in the peripheral region of the particle. They are caused by severe tensile stresses generated by the large plastic deformation in the interior of the particle. More details can be found in references [3,6] .

The phenomenon, that brittle materials, such as quartz deform mainly plastically as the particle becomes very small is very important for the comminution technology in terms of a grindability limit.

C.4 Agglomeration

If the particle is loaded further after fracturing, the fragments may re-agglomerate, particularly when they have built up a small mound instead of flying off. This special behaviour depends on the strength of the material, but, as a rule of thumb one observes that, the stronger the particle is, the larger is the stored elastic energy before fracturing, and the larger is the kinetic energy of the fragments. Limestone fragments, therefore, tend to agglomerate more than quartz fragments [8] .

During agglomeration energy is adsorbed by friction between the particles. The friction produces few fragments and little new surface [9] . The fracturing in the first phase of

loading is not separated sharply from the later agglomeration phase but there is a transition phase when both phenomena occur simultaneously. Experiments show, that the energy utilization i.e. the ratio of newly produced surface divided by the energy consumption, becomes worse as agglomeration enters the problem.

D. Similarity law of fracture mechanics in single particle crushing

The following quantities are very important in comminution

- 1) The ratio of newly produced surface to the volume S_V
- 2) The energy input per unit volume, called energy density E_V
- 3) The energy utilization $V_E = S_V/E_V$

So-called comminution laws have been formulated by Rittinger in 1867, by Kick in 1885 and by others which laws relate these quantities to particle size. They all are based on false or unrealistic physical assumptions. Any statement on fracture must be in accordance with fracture mechanics. Of course it is not practical to use fracture mechanics to predict the development of specific surface in beds of irregularly shaped particles, under stress but it is possible to derive relationships with the help of dimensional analysis.

D.1 Similarity law for physically identical materials

Particles of different size are compared and we assume that:

- 1) If the particles are geometrically similar then their size can be represented by one characteristic length x .
- 2) The particle material is homogeneous and isotropic.

- 3) The behaviour is purely elastic, excepting possibly microplastic deformations at the crack tip.
- 4) The deformations and the stress states are similar, before fracture occurs.
- 5) The fracture characteristics surely depend on
 - 1) the initial flaws l_i/x and their distribution $\phi(l_i/x)$ as a function of their location
 - 2) the maximum fracture energy $\beta_{max} = 1/2 G_c$, with G_c denoting Irwin's critical crack extension force
 - 3) the maximum crack velocity $V_{c,max}$ under definite stress conditions, for instance in a tensile strength experiment.

By "physically identical materials" we shall mean that all these properties are the same for otherwise different materials:

$$l_i/x = \text{const}, \beta_{max} = \text{const}, V_{c,max} = \text{const} \quad (1)$$

We now ask for conditions necessary to form similar fracture patterns as a result of which we can make a statement on the development of new surface. If the propagation of cracks is similar in particles of different sizes x , then any given fracture pattern generated during fracturing can be specified by a characteristic crack length l , so that the same fracture pattern is determined by the dimensionless value l/x . G is the specific crack extension energy or "crack extension force", associated with the crack length l/x . The dimensional analysis leads to

$$(G/E_V x) = f(l/x) \quad (2)$$

PL IX-142

Similar fracture pattern implies $l/x = \text{const}$, so that there follows

$$G/E_V x = \text{const} \quad (3)$$

For the critical crack length l_c/x and the associated critical crack extension force G_c , one may write, because of the similarity postulate (1), $l_c/x = \text{const}$ and $G_c/E_V x = \text{const}$ because of (2) and (3). The second of the assumptions (1) leads to $G_c = 2 \beta_{max} = \text{const}$ and so it follows that

$$E_V \cdot x = \text{const} \quad (4)$$

This is the condition for developing similar fracture patterns in particles of different size under the above assumptions.

For rapid crack propagation with $G > G_c$, the dynamic effects are very important. Changes in stress propagate with the speed of elastic waves so that the energy available at the tip of the crack becomes time-dependent. Now it should be assumed that for a given substance and a similar state of stress, the crack propagation speed is a unique function of G , i.e. constant at any position l/x . This assumption is supported by experiments, [10, 11], but should be tested further since it is so basic to the physics of fracture. The maximum crack speed depends on the stress distribution and is therefore, independent of the particle size. Since the speed of the elastic waves is also constant one can show that the similarity is satisfied during the development of the stress pattern and also for the dynamic stress distribution if the conditions (1) and (4) are fulfilled. When in particles of different size the fracture pattern is similar, the specific surface must obey the relation

$$S_V \cdot x = \text{const} \quad (5)$$

PL IX-142

It now follows for the energy utilization from (4) and (5) that

$$S_E = S_V/E_V = S_V x/E_V x = \text{const} \quad (6)$$

This formulard is identical with Rittinger's law which has been stated by him empirically and without any valid physical justification.

Of course the condition $l_i/x = \text{const}$ is not entirely realistic. On the contrary it should be expected that l_i/x is changing with particle size, presumably decreasing with increasing x .

D.2 Dimensional analysis for geometrically similar particles of different materials

The conditions (1) of chapter D 1 are maintained. But instead of a similar stress state equation 2, we assume now that only the boundary displacements caused by the tool have the same direction relative to the particle but may have different velocities v_d . The static and dynamic elastic behaviour is governed by the material properties, Young's modulus E , Poisson ration γ and the mass density ρ . For reasons of simplicity we assume that the maximum speed of elastic waves is that of the linear longitudinal wave $v_{el} = \sqrt{E/\rho}$. The velocity of the other types of waves are functions of v_{el} and γ . The breakage properties l_i/x , β_{max} and $V_{C,max}$ are assumed known.

Because in this case similar fracture patterns are not likely to develop we cannot ask for G as a function of $1/x$, but only for the result of fracturing namely for $S_V x$. The following quantities are to be taken in account:

$$S_V, E, \rho, \gamma, l_i, x, E_V, v_d, \beta_{max}, V_{C,max}$$

and the dimensional analysis results then in

$$S_V x = f \left(\frac{E_V}{E}, \frac{E_V x}{\beta_{max}}, \frac{V_{C,max}}{v_{el}}, \frac{v_d}{v_{el}}, \frac{l_i}{x}, \gamma \right) \quad (7)$$

For particles of the same material but different initial flaws l_i/x there follows

$$S_V x = f \left(\frac{E_V x}{\beta_{max}}, \frac{v_d}{v_{el}}, \frac{l_i}{x} \right) \quad (8)$$

The ratio v_d/v_{el} may be neglected for static and quasi-static conditions. In impact loading v_d is not an independent variable, since $E_V \sim v_d^2$, so that both for static stress states and for impact loading equation (8) simplifies to

$$S_V x = f \left\{ (E_V x/\beta_{max}), (l_i/x) \right\} \quad (9)$$

The function f is of course different for quasistatic and impact loading. The similarity conditions are then again $E_V x = \text{const}$ and $l_i/x = \text{const}$ as well as their distribution $\phi(l_i/x) = \text{const}$ as before so that one obtains (5) and (6).

D.3 Fracture behaviour of single particles and comparison with the similarity law

Before considering the behaviour of some select materials a few general remarks are necessary in advance.

- 1) The law of similarity has been deduced for the development of cracks, i.e. for the generation of new fracture surfaces. Normally the surfaces are measured after they have reacted with the surrounding humid atmosphere. Under constant material conditions the reactivity of the fresh surface depends on the local energy concentration at the crack tip, i.e. on G . In this case the similarity conditions (1), (3) and (4) state that the ratio of the new surface to final surface should also be constant. The reduction of fresh surface by reaction was investigated by Schwenk [12] .
- 2) Irregular particles are never geometrically similar. They also are not similarly deformed, nor are they

physically identical. Then, what is the sense of a similarity law? The answer is, of course, that the similarity laws cease to be applicable to tests on single particles. They only allow statistical statements for tests with a great number of particles. The experimental results discussed later are mean values for many particles.

- 3) It should be possible however, to check these similarity laws in principle with individual pieces of similar shape and initial flaw pattern, i.e. with $l_i/x = \text{const.}$ We have not yet made these experiments.
- 4) With irregularly shaped particles, E_V and $E_V x$ can be chosen arbitrarily, because fracturing of an irregularly shaped particle is a stepwise process. With a greater number of particles of the same size the mean of the newly created surface $S_V x$ is a smooth monotone function of the invested energy $E_V x$. The same is valid for impact loading. The influence of the initial flaws l_i/x may be smaller in this case, since many new flaws and fragments are produced. This would mean, that condition (1) is less important than condition (3) for satisfying the similarity law (4).

Quartz

In Fig. 12 the energy utilization has been plotted against particle size for compression, impact and drop weight crushing of quartz particles. The parameter $E_V x$ is the "energy investment" which must be constant for similar fracture patterns. Horizontal lines should be obtained when the similarity law is obeyed.

- 1) For the compression crushing of quartz particles the expected law is obeyed relatively well in the wide particle size range from 50 μm to 5 mm although the energie utilization tends to decrease slightly with

increasing particle size x . This is presumably due to the fact, that l_i/x is not strictly constant. The crack initiating flaws are certainly not 100 times larger in 5 mm quartz particles than in 50 μm ones. The fracture pattern is given, as a first approximation, by the energy investment $E_V x$. In a second approximation it is probable that the less favourable starting conditions of the cracks in the larger particles will be the governing factor. This might explain the trend towards a drop in the energy utilization with increasing x .

- 2) When quartz particles are crushed by compression, the energy utilization decreases with increasing energy investment E_V . Therefore the amount that is lost becomes greater due to increasing frictional losses as the fragments are stressed further. The constancy of the frictional losses at constant S_E and $E_V x$ - i.e. also at constant $S_V x$ - means that these losses are at all times proportional to the existing surface, which is physically plausible.
- 3) If plastic deformations were to play a significant part in the compression crushing of quartz particles, they would be expected to reduce the energy utilization. Because no reduction in the energy utilization has, in fact, been found with particles down to 50 μm , it follows that plastic deformations play a minimal part. This is in agreement with the load-displacement curves measured by Steier [6] .
- 4) Impact crushing of quartz (Fig. 12) leads to a smaller amount of energy utilization - at the same $E_V x$. This must be due to the completely different dynamic stress pattern and may be due to the greater proportional loss in the form of kinetic energy.

Impact comminution also involves secondary crushing by mutual impact of the fragments. Reiners [13] found

that the fragments of impacted glass balls which fly off laterally may reach very high speeds, e.g. 1500 m/s for an impact speed of 380 m/s. The reduction in the energy utilization as $E_v x$ rises can be explained by the increase in both the primary and the secondary losses. The reduction with increasing particle size but at constant $E_v x$ suggests that the development of the surface in impact crushing depends more on the initial conditions than in the case of compression crushing.

Limestone

Another thoroughly investigated material is limestone (Fig. 13). It shows a behaviour different from that of quartz, and one that is typical for the weaker brittle materials.

- 1) In compression crushing of limestone the energy utilization increases with increasing particle size and decreases with increasing energy investment $E_v x$. Both are due to agglomeration which has been observed experimentally and on which we have already commented. Agglomeration becomes more pronounced as more fine fragments are produced, i.e. the smaller the particle size and the larger the energy investment $E_v x$. It is also possible that some plastic deformation, which increases with decreasing particle size, may play a part.
- 2) In impact crushing the dependence on particle size is reversed. Less new surface is produced, than in compression crushing, i.e. less fine fragments are produced. Here agglomeration may be less important and the energy utilization decreases as the particles become larger. As with quartz, this could be explained with the conjecture that the initial flaw distribution l_i/x does not remain constant.

Final remarks

All these interpretations are still rather hypothetical in nature. But they do seem to give an orientation for a combined interpretation of fracture physics, fracture mechanics, and single particle crushing.

The representation of experimental data in the similarity graph (figure 13, 14) helps us to understand the material behaviour based on fracture physics. It provides an additional criterion which is most instructive, particularly in connection with another graph, e.g. S_E versus E_v as it is discussed in another paper [14] .

Acknowledgment

This paper is based on many investigations, which have been carried out in the "Institut für Mechanische Verfahrenstechnik der Universität Karlsruhe", see references [1-3, 5-10, 14] . I am very grateful to all co-workers, who, also by discussion, have contributed to the progress of our knowledge.

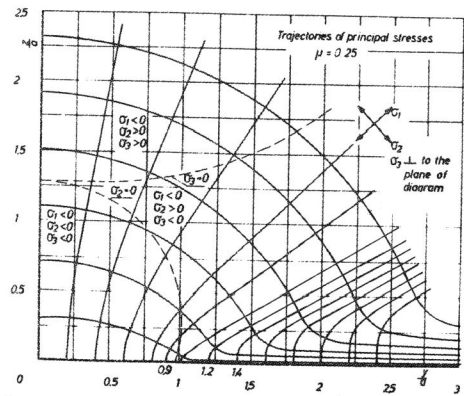


Fig. 1 Trajectories of the Hertz-Huber-stress field [from ref. 3]

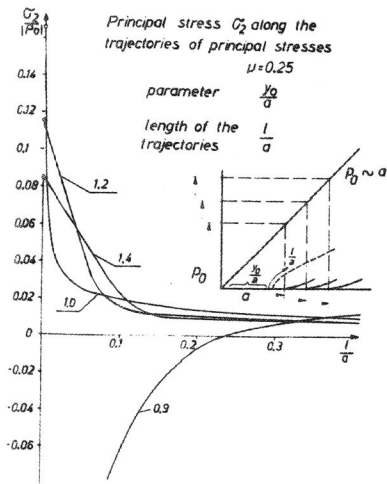


Fig. 2 Principal stress σ_2 perpendicular to the trajectory of the principal stress σ_1 versus path length; parameter is the distance (y_0/a) of the starting point from the center of the contact circle [from ref. 3]

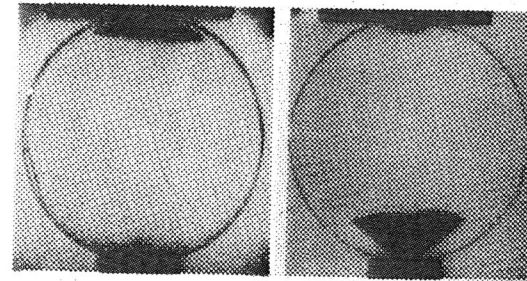


Fig. 3 Cone cracks; left: surface near cone crack right: center near cone crack [from ref. 3]

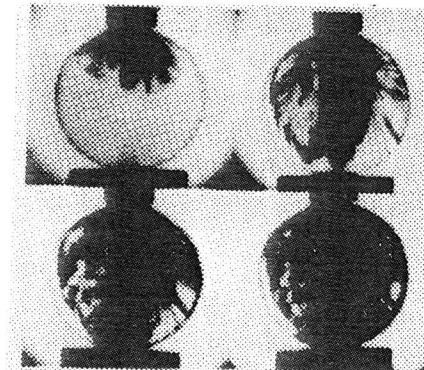


Fig. 4 High-speed photographs of the fracturing of a glass sphere; time after triggering: 2.2; 6.5; 10.7; 15.3 μ s [from ref. 3]

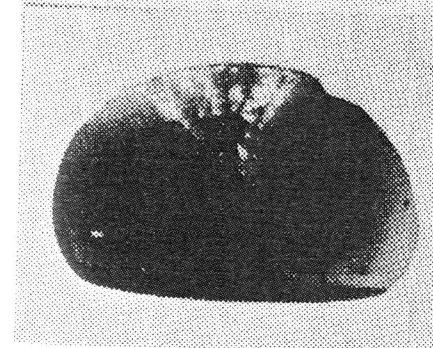


Fig. 5 Cone-shaped region beneath the contact area in a splitted wax half sphere which was deformed plastically [from ref. 3]

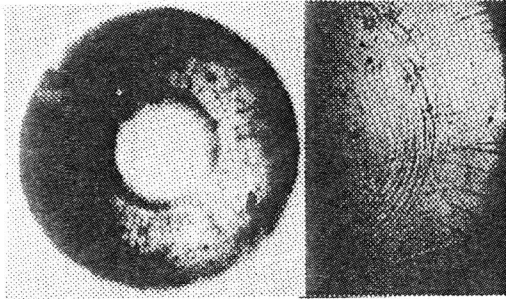


Fig. 6
Ring-cracks and meridional cracks around the contact area of a polystyrene sphere [from ref. 3]

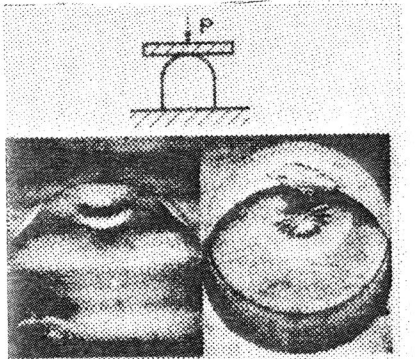


Fig. 7
The begin of meridional cracks in PMMA caused in a cooled specimen (liq. nitrogene) by compression [from ref. 3]

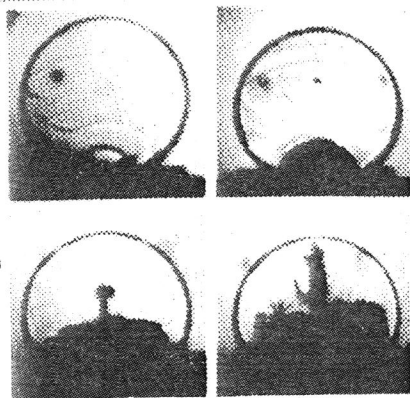


Fig. 8
High-speed photographs of the impact of a PMMA-disc; time distance between the frames about 3 μ s [from ref. 5]

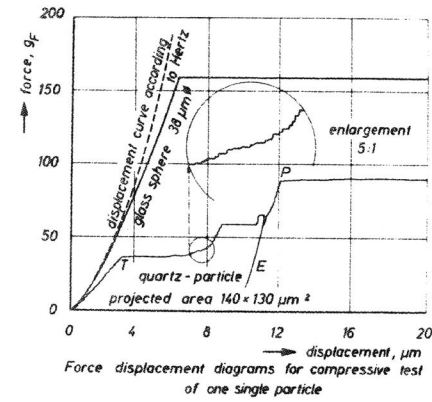


Fig. 9
Load-displacement-curves from compression tests of a 130 μ m-quartz particle and a 38 μ m-glass sphere

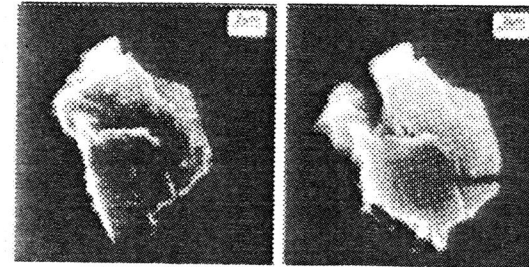


Fig. 10 Scanning electron microscope pictures of a 9 μ m-limestone particle before and after loading [from ref. 6]

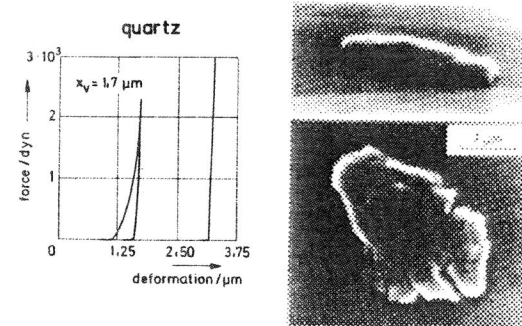


Fig. 11 Compression test of a 1.7 μ m quartz particle; left: load-displacement-curve, right: scanning electron microscope picture after loading [from ref. 6]

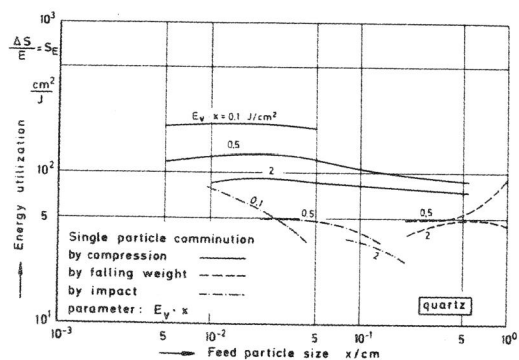


Fig. 12 Similarity plot: energy utilization at compression and impact tests with quartz particles; parameter is the specific energy times particle size: $E_v \cdot x$

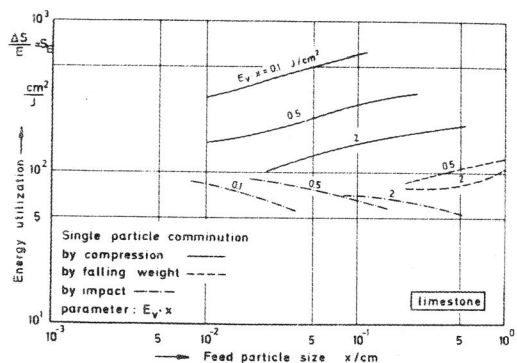


Fig. 13 Similarity plot: energy utilization at compression and impact test with limestone particles; parameter is the specific energy times particle size: $E_v \cdot x$

PL IX-142

References

- 1 H. Rumpf Chemie-Ingenieur-Technik 37 (1965) 187/202
- 2 H. Rumpf Aufbereitungstechnik 7 (1966) 421/435
- 3 H. Rumpf, K. Schönert Drittes Europäisches Symposium Zerkleinern, Cannes 1971, Dechema-Monographien Bd. 69, 1972, Vortrag I-2
- 4 T.R. Wilshaw, N.E.W. Hartley s. Reference 3, Vortrag I-1
- 5 H.H. Gildemeister, K. Schönert s. Reference 3, Vortrag I-8
- 6 K. Steier Diss. Universität Karlsruhe, 1972
- 7 K. Steier, K. Schönert s. Reference 3, Vortrag I-6
- 8 K. Schönert, K. Steier Chemie-Ingenieur-Technik 43 (1971), 773/777
- 9 W.v.d. Ohe Chemie-Ingenieur-Technik 39 (1967) 5/6, 357/364
- 10 K. Schönert, H. Umhauer, W. Klemm Fracture 1969, Proceedings of the Second. Int. Conf. on Fracture, Brighton, April 1969, Chapman and Hall Ltd.
- 11 F. Kerkhof, H. Richter Wissenschaftl. Bericht Nr. 5, 1967, Ernst-Mach-Institut, Freiburg
- 12 W. Schwenk s. Reference 3, Vortrag I-4
- 13 E. Reiners Forsch. Ber. des Landes Nordrhein-westfalen Nr. 1059 (1962)
- 14 H. Rumpf will be published in Powder Technology

PL IX-142